Microchimica Acta
https://doi.org/10.1007/s00604-019-3356-2

ORIGINAL PAPER

Split aptamer-based detection of adenosine triphosphate using surface enhanced Raman spectroscopy and two kinds of gold nanoparticles

Chunyang Zhou[1] · Zhi Yu[1] · Weili Yu[1] · Huiwen Liu[2] · Hao Zhang[2] · Chunlei Guo[1,3]

Received: 21 January 2019 / Accepted: 2 February 2019

Abstract

An ultrasensitive and highly selective method is described for the determination of adenosine triphosphate (ATP) via surface-enhanced Raman scattering (SERS). Two split aptamers are used for specific recognition of ATP. They were attached to two SERS substrates. The first was placed on a nanolayer of gold nanoparticle-decorated graphene oxide (GO/Au3), and the other on gold nanoparticles (Au2). When ATP is introduced, it will interact with the split aptamers on the gold nanostructures to form a sandwich structure that brings the GO/Au3 nanolayer and the Au2 nanoparticle in close proximity. Consequently, the SERS signal, best measured at 1072 cm^{-1}, is strongly enhanced. The sandwich structure also displays good water solubility and stability. Under optimized conditions, the SERS signal increases in the 10 pM - 10 nM ATP concentration range, and the limit of detection (LOD) is 0.85 pM. The method was applied to the determination of ATP in spiked human serum, and the LODs in serum and buffer are comparable. In our perception, the method has a wide scope in that numerous other aptamers may be used. This may result in a variety of other highly sensitive aptasensors for use in in-vitro diagnostics.

Keywords Sandwich nanostructure · Biosensor · Graphene oxide · SERS · Human serum · Aptasensor · Diagnostics

Abbreviations

ATP Adenosine Triphosphate
PATP p-aminothiophenol

Introduction

ATP regulates many biological pathways, and it is responsible for intracellular energy transfer that in turn controls several cellular functions. A decreased level of ATP can lead to several symptoms such as ischemia, Parkinson's disease, hypoglycemia and some types of malignant tumors [1–3]. Therefore, the development of ATP biosensors with high sensitivity is critical to human health.

Aptamers are artificial single-stranded DNA or RNA screened by systematic evolution of ligands via exponential enrichment, which can greatly improve the sensitivity of biosensor [4]. It possesses exceptional binding affinity and specificity to their antigen target. In addition, unique properties such as higher purity, flexible modification and lower cost of production support their suitability for biomolecules determination. Since it was discovered in the 1990s, many biosensors rely on aptamers to achieve ultra-high sensitivity have been developed [5]. Nowadays, the highly sensitive aptamer biosensor technologies has been applied in numerous applications, including the detection of DNA/RNA or antigen/antibody for the measurement of clinical parameters, pathogens, and tumor cells [6–9]. Interestingly, when a single ATP aptamer splits into two fragments, it will equilibrate between

Electronic supplementary material The online version of this article (https://doi.org/10.1007/s00604-019-3356-2) contains supplementary material, which is available to authorized users.

✉ Chunyang Zhou
cyzhou@ciomp.ac.cn

✉ Chunlei Guo
guo@optics.rochester.edu

[1] The Guo China-US Photonics Laboratory, Changchun Institute of Optics, Fine Mechanics and Physics, Chinese Academy of Sciences, Changchun, Jilin 130033, People's Republic of China

[2] State Key Laboratory of Supramolecular Structure and Materials, College of Chemistry, Jilin University, Changchun 130012, People's Republic of China

[3] The Institute of Optics, University of Rochester, Rochester, New York 14627, USA

Published online: 20 March 2019

its two dissociated parts and a folded, associated complex [10]. If the target binds the complex with high affinity, the presence of the target will drive the equilibrium toward the formation of this complex. Therefore, by using two split aptamers instead of a single aptamer to specifically identify the target, the targeting accuracy can be greatly improved. Based on these facts, we utilized this mechanism to create a sandwich assay by splitting the ATP aptamer into two fragments for the construction of ATP biosensor with high sensitivity and selectivity.

Surface-enhanced Raman scattering (SERS) performs powerful ability to enhance Raman signals, which can be up to 10^6–10^{14} orders of magnitude [11–14]. In addition, it has promising sensitivity and spatial resolution. Based on these characteristics, SERS can be widely used as a powerful technique in biosensing and imaging applications [15, 16]. Because of its narrow-band Raman spectral signature and wide excitation wavelength, it performs the multiplexing detection capability with laser excitation. Such technology also possesses the ability of single-molecule detection due to its unique molecular fingerprinting information [17, 18]. These large enhancements are predominant attributed to the concentration of electromagnetic (EM) optical fields at "hot spots". Such feature is considered to be Plasmon-based effect and is very important to achieve the high sensitivity of SERS detection. Most often, the "hot spots" consist of nanoscale junctions and interstices in metal nanomaterials such as nanoparticle dimers and aggregates [19]. Thus, there are still many challenges to realize ultrasensitive chemical/biological assay technique based on a reliable SERS platform.

Therefore, we will strive to synthesis suitable nanomaterials to construct a SERS-based reaction platform with high response. Some investigations have revealed that graphene-based nanosheets loaded with various nanoparticles can improve SERS efficiency compared to the use of plasmonic nanostructures alone [20, 21]. As one of the most important graphene derivatives, graphene oxide (GO) has been widely used as a carrier for the preparation of nanocomposites due to its distinct physical and chemical properties [22]. Metal nanoparticles, such as colloidal gold nanocrystals, are a class of plasmonic materials that have been widely used in surface-enhanced spectroscopy, optical imaging and biosensing [23, 24]. The key characteristic of metal nanostructures is that the collective and surface plasmon excitation of free electrons can enhance the EM near its surface by many orders of magnitude [25]. Several works have shown that nanoscale junctions or nanogaps between two or more metal nanoparticles are associated with plasmonic "hot spots" and then enhance the SERS signal [26]. Based on the above facts, for the first time, we developed a self-assembly sandwich nanostructure as unique SERS assay platform for the sensitive detection of ATP. The assay platform is consist of the complex of grapheme oxide/AuNP (GO/AuNP) and gold nanoparticle monomer (AuNP). The first one was attached to one of the split aptamers (apt1), and the second one was modified with another split aptamer (apt2) via the Au-S bond. The ATP-induced association of the two fragments with the complex formed between GO/AuNPs and gold nanoparticle monomers mainly controls the plasmonic coupling and the EM field. This results in the highly sensitive and selective ATP assay described here.

Materials and methods

Materials

Graphite and hydrogen tetrachloroauric acid ($HAuCl_4 \cdot 3H_2O$) were purchased from Sigma-Aldrich and used without further purification. Graphene oxide was synthesized from graphite powder by a modified Hummers method [27]. DNAs were purchased from Sangon Biotechnology Co., Ltd. (www.sangon.com). Alpha fetoprotein (AFP) antigen and antibody, ATP, cytidine triphosphate (CTP), uridine triphosphate (UTP), adenosine diphosphate (ADP), adenosine monophosphate (AMP) and guanosine triphosphate (GTP) were purchased from Sigma-Aldrich (sigmaaldrich.biogo.net). Other chemicals were of reagent grade and were used without further purification. The oligonucleotides were dissolved in water as stock solution and quantified by UV − Vis absorption spectroscopy with the following extinction coefficients (ε260 nm, M^{-1} cm^{-1}): A = 15,400, G = 11,500, C = 7400, T = 8700. The sequences of the designed aptamers are as follows:

SH-aptamer1: 5′- SH-ATACC TGGGG GAGT A TATAA T-3'
SH-aptamer2: 5'-SH- ATTAT AGCGG AGGAA GGTAT-3'

Characterization

The TEM images were recorded on JEM-2010 transmission electron microscope under a working voltage of 200 kV. Raman spectroscopy was conducted using a Labram HR Evolution Raman spectrometer (Horiba Scientific) (objective: 50×, NA = 0.50, grating: 1800, measurement mode: confocal.). The laser operating at λ = 785 nm was used as the excitation source with a laser power of about 9.6 mW. The integration time was set as 10 s. UV − Vis absorbance measurements were performed on a Cary Series Scan UV/Vis/NIR Spectrophotometer (Agilent Technologies). A Cary Eclipse Fluorescence Spectrophotometer (Agilent Technologies) was used to collect the fluorescence emission spectra of fluorophore modified aptamers in Tris-HCl buffer (20 mM Tris-HCl, 200 mM KCl, 10 mM $MgCl_2$, pH 8.0) under room temperature.

Preparation of gold nanoparticles (AuNPs) and GO/AuNP

The AuNPs with different diameters were prepared as previously reported [28]. All glass wares applied in this experiment were completely cleaned in aquaregia ($HCl:HNO_3 = 3:1$), rinsed in doubly distilled water, and dried prior to use. In a 100 mL conical flask, 50 mL of 1 mM $HAuCl_4$ in ultrapure water was heated to boil with vigorous stirring, followed by rapid addition of different amounts of sodium citrate to control the size of AuNP. The solution turned deep blue in a short moment, and the final color changed to wine-red after 60s. The boiling state lasted for an additional 15 min, then the heating source was removed, and the colloid solution was stirred for another 30 min. The resulting AuNP solution was stored in dark bottles at 4 °C.

To prepare the self-assembled GO/AuNP nanocomposites, $HAuCl_4$ (500 μL, 1%) was added into the aqueous solution of 24.5 mL, followed by the addition of GO (625 μL, 1 mg·mL^{-1}). The solution was kept in a room temperature environment for 30 min and then heated to 80 °C. Then the various amounts of sodium citrate was added into it dropwise and cultivated for 60 min. The GO/AuNP nanocomposite was successfully synthesized after centrifuged (5000 rpm, 15 min) several times to remove the redundant AuNP.

Optimization of method

The following parameters were optimized: (a) pH value; (b) Mg^{2+} concentration; (c) temperature; (d) size of AuNPs; (e) apt1 concentration. Respective data and Figures are given in the Electronic Supporting Material. The following experimental conditions were found to give best results: (a) Best pH value: 7; (b) Mg^{2+} concentration: about 1 mM; (c) Optimal temperature: 37 °C; (d) size of AuNPs: 25 nm; (e) apt1 concentration: 50 nM for GO/Au1, GO/Au2 and GO/Au4, and 80 nM for GO/Au3.

Assay procedure for SERS detection of ATP

The optimized concentrations of apt1 (80 nM) and apt2 (100 nM) were added to GO/Au3 nanolayer and Au2. Then, the solutions were centrifuged at 8000 rpm for 10 min to remove excess apt1 and apt2 and re-dispersed into H_2O. Different concentrations of ATP were added into the mixture of GO/AuNP/apt1 nanolayer and AuNP/apt2 and incubated for 40 min. The resultant samples were then used for SERS measurements. SERS measurements were performed using Labram HR Evolution Raman spectrometer with 9.6 mV laser power and the acquisition time was 10 s for all SERS spectra. Each sample measurement was performed at least for three times.

Results and discussion

Mechanism of the assay

The fabrication processes of the SERS biosensor are shown in Scheme 1 based on the platform of the complex of GO/AuNP nanolayer and AuNP monomer. Initially, different kinds of the complex of GO/AuNP (GO/Au1, GO/Au2, GO/Au3 and GO/Au4) nanolayer and AuNP monomer (Au1, Au2, Au3 and Au4) were synthesized separately. Then, the hydrosulphonyl modified aptamer1 (apt1) was stable anchored on the surface of GO/AuNP nanolayer based on the Au-S bond, followed by the addition of p-aminothiophenol (PATP), which was chosen as the probe molecule to investigate the SERS activities. Furthermore, the AuNP monomer was coated with hydrosulphonyl modified aptamer2 (AuNP/apt2) via Au-S bond. The aptamers (apt1 and apt2) are anchored on the surface of GO/Au3 nanolayer and Au2, respectively. They form the two split fragments of the single ATP aptamer. An equilibrium is formed between the two dissociated parts and the associated complex [10]. Therefore, before the addition of ATP to the sandwich reaction platform, different parts of the platform existed randomly without connection. When ATP was added to the platform, it can bind to both apt1 (anchored on the surface of GO/AuNP nanolayer) and apt2 (connected with AuNP monomer). The distance between two kinds of AuNP from the complex of GO/AuNP and AuNP monomer became closer as a result. Thus, the forming nanoparticle dimers with nanoscale gaps can induce SERS signal, which is the result of "hot spot" formation [18]. By capturing the SERS signals under different conditions, the biosensing of ATP with high sensitivity was achieved.

Characterization of the sandwich nanostructure

To form the sandwich GO/AuNP/apt1 + ATP + AuNP/apt2 structure for the successful detection of ATP in human serum, the pH value, Mg^{2+} concentrations and reaction temperature were optimized firstly as shown in Fig. S1. The HR-TEM morphologies of AuNP and GO/AuNP are shown in Fig. 1a, b. When they were mixed together after connecting with apt1 and apt2, the AuNP dimers appeared on the surface of GO after the addition of ATP, as shown in the circled portions in Fig. 1c. Such conjugation of GO/AuNP/apt1 with AuNP/apt2 by ATP was further confirmed by UV-Vis spectroscopy as shown in Fig. 1d. The black and red curves of the absorption peaks represented the AuNP/apt2 and GO/AuNP/apt1, respectively. The locations of the two absorption peaks remained the same due to the optical absorption peak of GO in NIR region can not be observed even though it displayed a broad UV-Vis absorption [29]. When they conjugated with each other after the addition of ATP, the absorption peak of GO/AuNP/apt1 + ATP + AuNP/apt2 showed a certain shift (blue curve) in Fig.

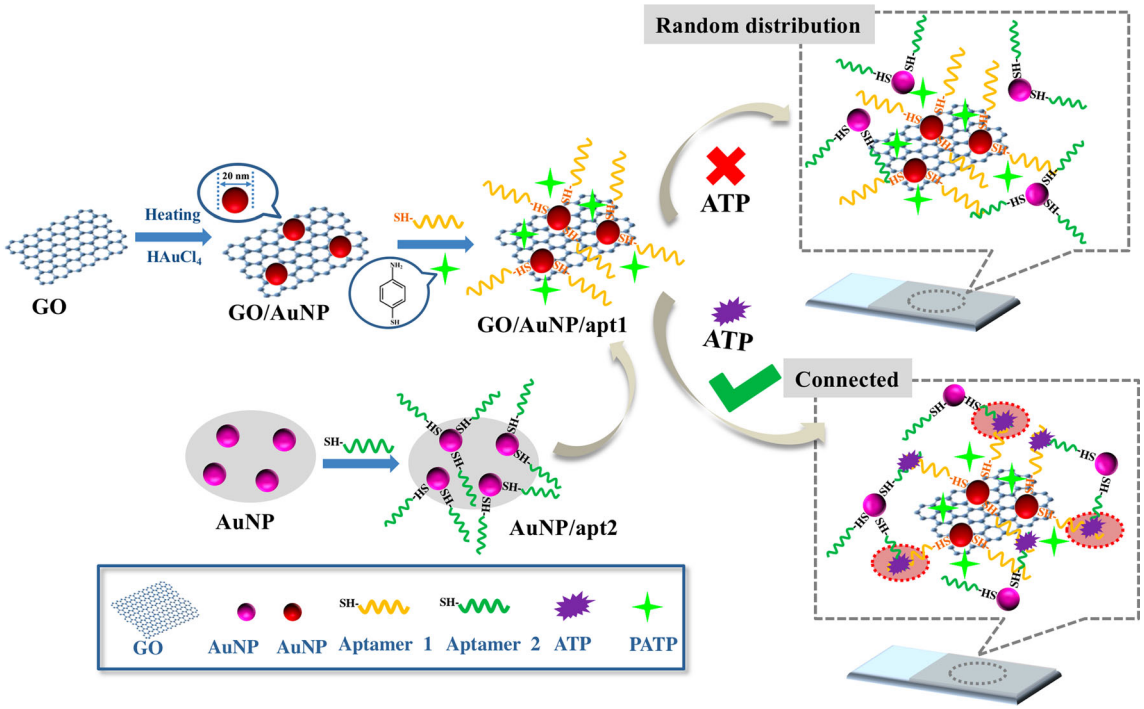

Scheme 1 The schematic illustration of the sandwich assay SERS detection of ATP based on the GO/AuNP/apt1 nanolayer and AuNP/apt2

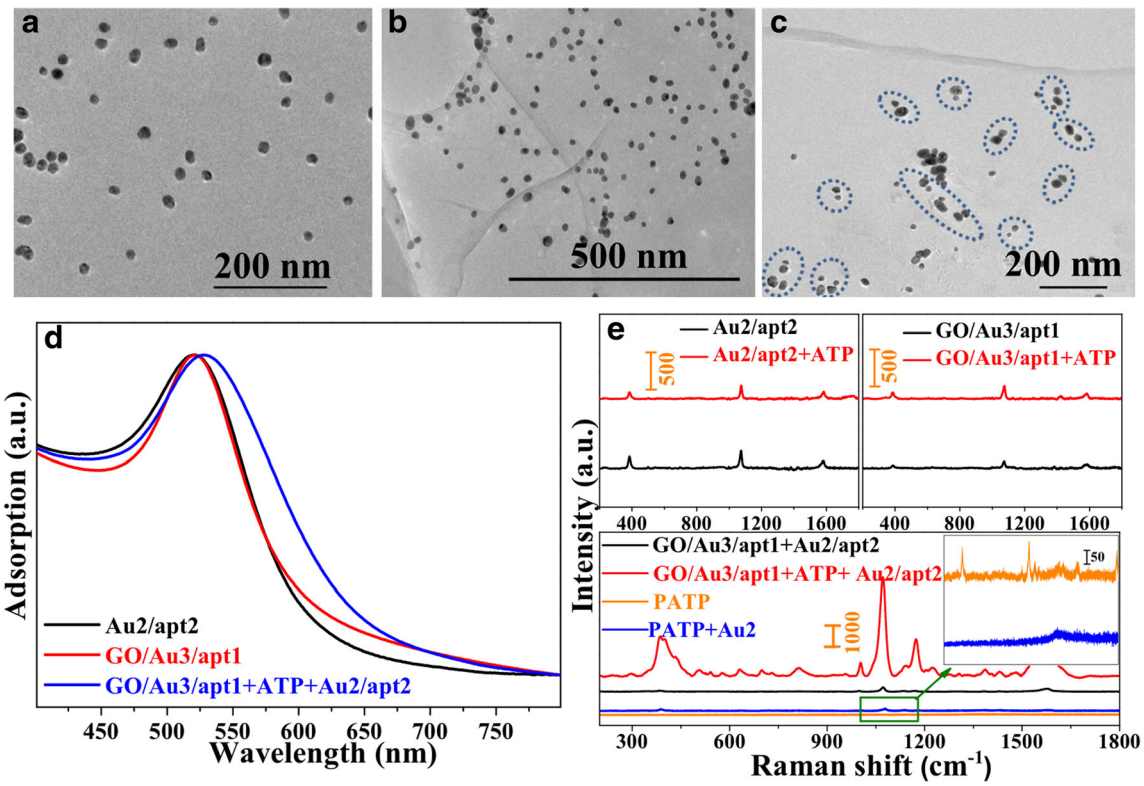

Fig. 1 HR-TEM images of (**a**) AuNPs monomer, (**b**) GO/AuNP nanolayer and (**c**) the sandwich GO/AuNP/apt1 + ATP + AuNP/apt2, which were highlighted in the dotted line. **d** The UV-Vis spectra of AuNP, GO/AuNP and the sandwich GO/AuNP/apt1 + ATP + AuNP/apt2. **e** Comparison of SERS spectra of the samples on the ITO before and after the addition of ATP. Samples for comparison include AuNP/apt2, GO/AuNP/apt1 and sandwich GO/AuNP/apt1 + ATP + AuNP/apt. Inset was the SERS signal of PATP probe before and after the addition of AuNP

1d. In addition, the obvious SERS signal was also displayed after the formation of the sandwich structures shown in Fig. 1e. The two parts of the platform of GO/AuNP/apt1 and AuNP/apt2 showed weak SERS signals before and after the addition of ATP compared to the situation of GO/AuNP/apt1 + ATP + AuNP/apt2. In Fig. 1e, by comparison with the SERS probe of PATP inset, which had a weaker SERS signal after adding AuNP monomer. According to the facts above, the detection of ATP based on SERS have been successfully achieved with the application of sandwich nanocomposites.

In order to detail and accurately demonstrate the important role of each component in enhancing the SERS signal in this work, first of all, we demonstrated the key role of the AuNP monomer that conjugated with apt2. If the role of AuNP monomer was removed from the sandwich structure of GO/AuNP/apt1 + ATP + AuNP/apt2 as shown in Fig. 2a, almost no SERS signal was observed after the addition of ATP to the mixture of GO/AuNP/apt1 and apt2. Without AuNP monomer, the critical "hot spot" can not be formed to enhance the SERS. Therefore, this phenomenon has fully proved the AuNP monomer in the structure of AuNP/apt2 played a significant role on enhanced SERS signal. Secondly, when the GO was removed from the sandwich structure of GO/AuNP/apt1 + ATP + AuNP/apt2, only a small change was observed before and after adding ATP to the mixture of AuNP/apt1 and AuNP/apt2 as shown in Fig. 2b. Such phenomenon attributed to the GO, as a support of nanomaterial, can not only load as many AuNP as possible, but also provided more opportunities of "hot spots", showing the indispensable role of GO in the sandwich structure. Finally, it is necessary to demonstrate the necessity of the AuNP in the GO/AuNP/apt1 nanolayer. From the change of SERS signals, after the addition of ATP to the mixture of GO/apt1 and AuNP/apt2, it showed little difference compare to the SERS signal without ATP in Fig. 2c. Thus, these results have fully demonstrated the crucial role of each component in the sandwich GO/AuNP/apt1 + ATP + AuNP/apt2 for realizing ATP detecting with high sensitivity.

In order to choose an optimal size of AuNP, which can lead to a higher SERS signal, different sizes of AuNP were synthesized as shown in Fig. 3a. Before optimizing the size of the AuNP that belongs to AuNP/apt2, we first optimized the concentrations of AuNP that grown on the surface of GO nanolayer as shown in Fig. S2 and Fig. S4. After comparison, the GO/Au3/apt1 that obtained AuNP-3 (Au3) was proved to be the best performer for SERS detection of ATP as shown in Fig. S5 and Fig. S6. In the next stage, the different size of AuNP that belongs to AuNP/apt2 was synthesized by varying the concentration of chloroauric acid and the morphologies were determined by TEM shown in Fig. 3a. The diameters of the AuNP were around 50, 25, 15 and 10 nm, respectively. The size distributions of the Au1-Au4 are shown in Fig. S4. Figure 3b showed the UV-Vis spectra of the corresponding different AuNP solutions with maximum peak locations at 541, 531, 526 and 520 nm, respectively. Then, the concentration of apt2 that anchored on the surface of AuNP should be certain. The 6-carboxyfluorescein (FAM, emission max at 521 nm) and hydrosulphonyl modified apt2 was used to connect with AuNP by Au-S bonds. The FAM-labeled apt2 was used when placed on the surface of AuNPs, its fluorescence is quenched because of surface energy transfer between the FAM and the AuNPs [30]. Based on the fluorescence intensity of FAM, as shown in Fig. 3c, the optimized concentrations of apt2 were confirmed to be 50 nM for Au1, Au3 and Au4, and

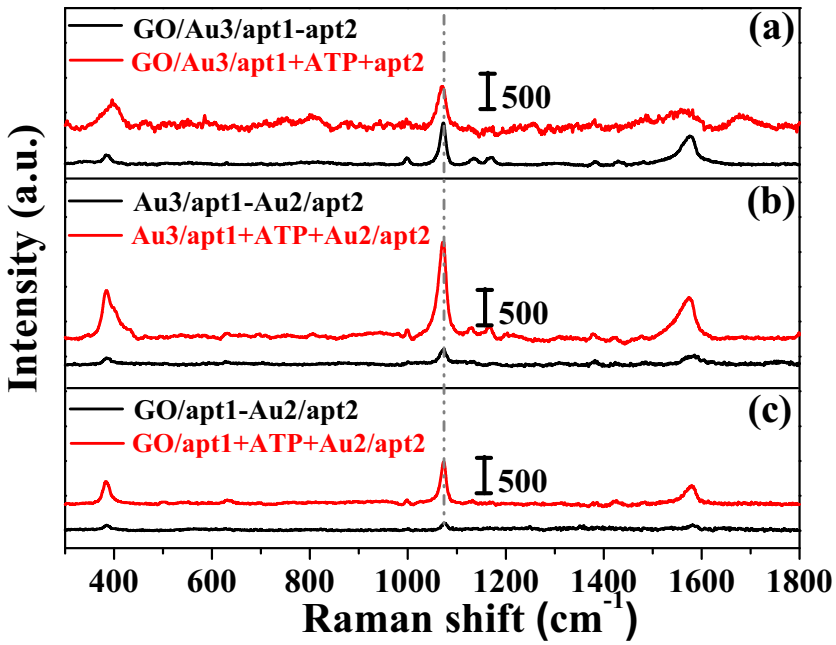

Fig. 2 Comparison of SERS signal of different substances before and after the addition of ATP. The comparison of peak intensities at 1072 cm^{-1}. The concentration of ATP used in the experiment was 50 nM. **a** when AuNP monomer was removed from the sandwich GO/AuNP/apt1 + ATP + AuNP/apt2, **b** when GO was removed from the sandwich GO/AuNP/apt1 + ATP + AuNP/apt2 and (**c**) when AuNP in GO/AuNP/apt1 was removed from the sandwich structure

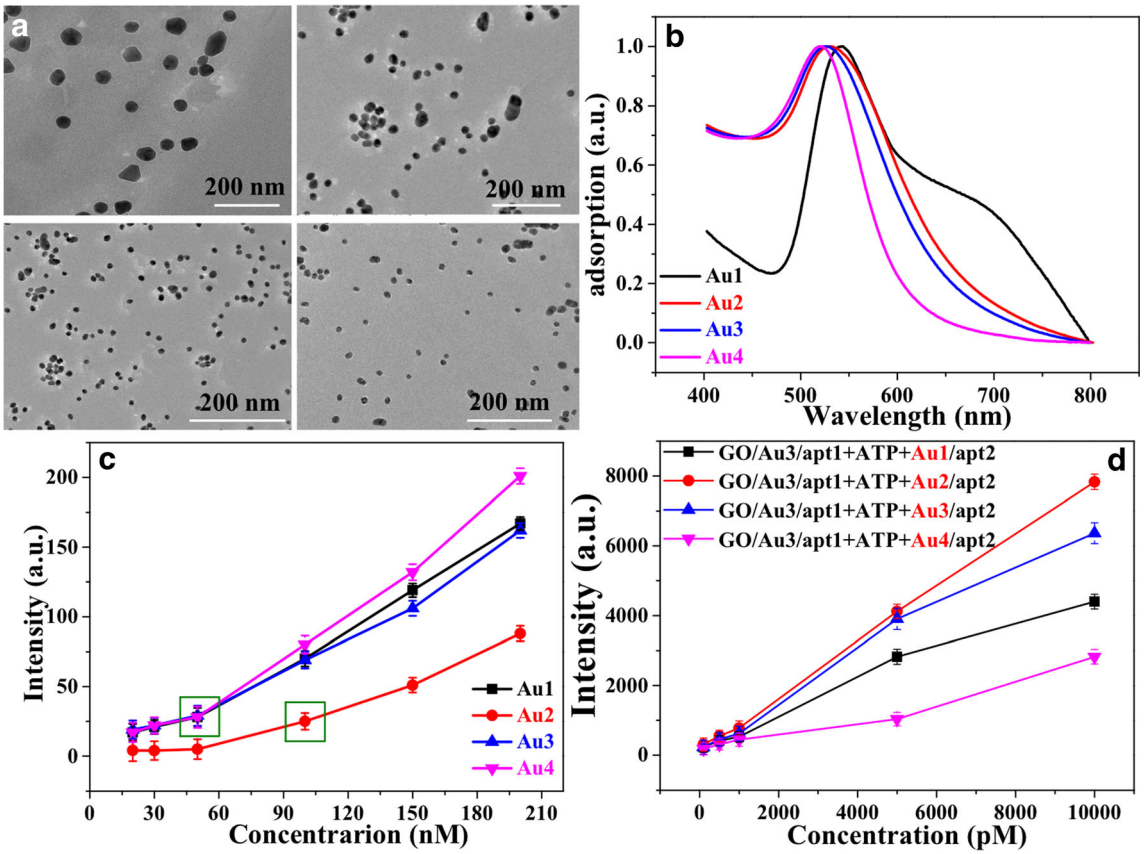

Fig. 3 **a** The TEM of Au1-Au4 with different diameters were around 50, 25, 15 and 10 nm, respectively. **b** The corresponding absorption spectrum of Au1-Au4. **c** The comparison of FAM fluorescence intensities on the surface of Au1-Au4. When the FAM-labeled apt2 was anchored on the surface of Au1-Au4, the FAM fluorescence can be quenched. **d** The comparison of calibration plots of SERS signals of the sandwich GO/Au3/apt1 + ATP + Au2/apt2. The comparison of peak intensities at 1072 cm^{-1}

100 nM for Au2, showing the Au2 with the greatest surface area connects with apt2 and regarded as the gold standard (its property for the SERS detection of ATP compared with the sandwich structure of GO/Au2/apt1 + ATP + Au2/apt2 are shown in Fig. S7). After that, the calibration plots of SERS signal on detecting ATP by GO/Au3/apt1 nanolayer mixed with different size of AuNP(1–4)/apt2 were compared as shown in Fig. 3d, from which we can determine that the LOD of each condition were 19 pM for GO/Au3/apt1 + ATP + Au1/apt2, 0.85 pM for GO/Au3/apt1 + ATP + Au2/apt2, 9 pM for GO/Au3/apt1 + ATP + Au3/apt2 and 35 pM for GO/Au3/apt1 + ATP + Au4/apt2. Thus, the optimized size of AuNP2/apt2 (Au2/apt2) showed the highest sensitivity of ATP with the best SERS signal in the sandwich structure of GO/Au3/apt1 + ATP + Au2/apt2. Such optimized conditions were chosen to use during this work.

Sensitivity of the assay

The SERS measurements of ATP bound to split aptamers with different concentrations were carried out as shown in Fig. 4a. We first operated the experiment by measuring the SERS intensity of the mixture of GO/Au3/apt1 and Au2/apt2 without ATP as the control (black curve with 0 pM in Fig. 4a), which showed a very weak SERS signal. When ATP was added, the SERS signal was obviously enhanced and went higher with the increased concentration of ATP. The response of the SERS intensity at 1072 cm^{-1} was plotted as a function of the ATP concentration shown in Fig. 4b. The limit of detection (LOD) by this SERS biosensor, which was defined as three times the standard deviation of the blank, was determined to be 0.85 pM. The SERS biosensor developed in this work showed a very low LOD compared to other results with different aptamer-based methods in detecting ATP summarized in the Table S1, which was first due to the unique shape of the AuNP that was stable immobilized on the surface of GO, fully connecting the split apt1 and providing the foundation for the detection of ATP. Second, the sandwich AuNP dimers were immobilized in proximity distance between them on the GO surface by utilizing the rigid feature of split aptamers, forming the "hot spots" between them and leading to significant enhancement of the local electromagnetic field. Third, the split DNA aptamers showed a high affinity with ATP.

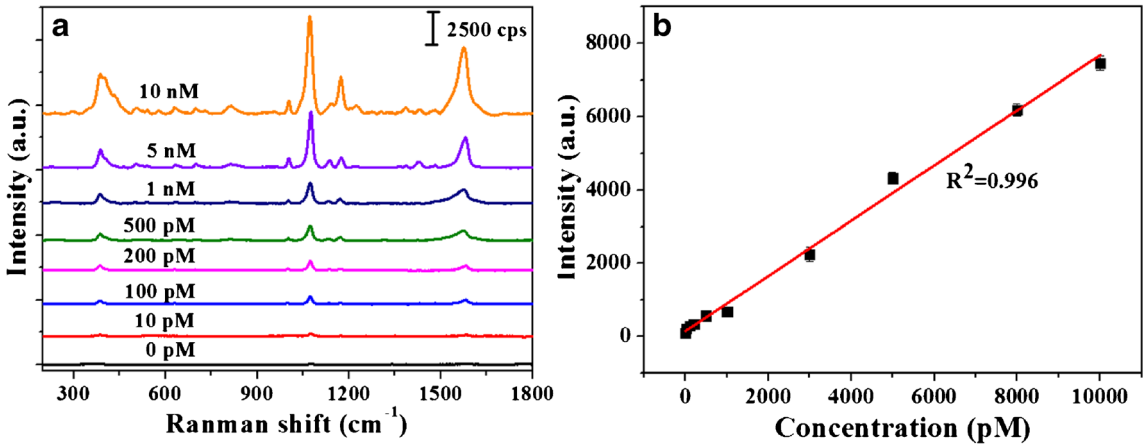

Fig. 4 SERS spectra (**a**) and calibration plot (**b**) of the aptasensor for ATP at different concentrations. The corresponding peak intensities were at 1072 cm^{-1}. The error bars represent the standard deviations of three independent measurements. The comparison of peak intensities at 1072 cm^{-1}

Specificity for ATP detection

The above results demonstrated the feasibility of detecting the presence of ATP in standard solutions with this SERS-based aptasensor. In order to evaluate the specificity of the SERS biosensor toward ATP, control experiments were conducted by incubating the SERS assay in the solutions containing glucose, thrombin, peptide antigen and antibody, Na^+, K^+, GTP and CTP, which are the basic building blocks in the blood. The concentration of ATP was 10 nM, and other individually measured targets were at the same concentration of 100 nM. As shown in Fig. 5, the signal intensity increased significantly with the addition of ATP, while there were no obvious changes in SERS intensities for other targets. Among them, it can be seen that the GTP and CTP induced a negligible response of the SERS signal although they have chemical structures similar to ATP [31]. Such facts demonstrated the established aptasensor obtained good selectivity and there was no serious cross reaction for the detection of ATP.

Application in human serum samples

In order to evaluate the analytical reliability and accuracy of the SERS-based aptasensor in practical applications, the utility of the sandwich GO/Au3/apt1 + ATP + Au2/apt2 for the detection of ATP was performed in human serum samples. The experiment was used as a simulation of clinical samples. Compared to SERS signal of the reaction platform without ATP, the detected concentrations of ATP in serum showed good detection performance and were almost consistent with those determined in buffer as shown in Fig. 6. This indicates that this assay represents a promising method for clinical applications. As shown in Table 1, all of the recoveries obtained for different ATP

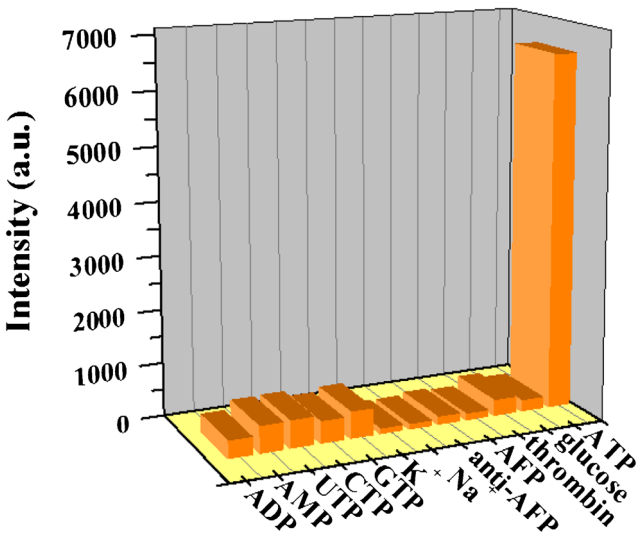

Fig. 5 Evaluation of the selectivity of the SERS biosensor at different target analytes. The concentration of ATP is 10 nM, and other targets are 100 nM. The comparison of peak intensities at 1072 cm^{-1}

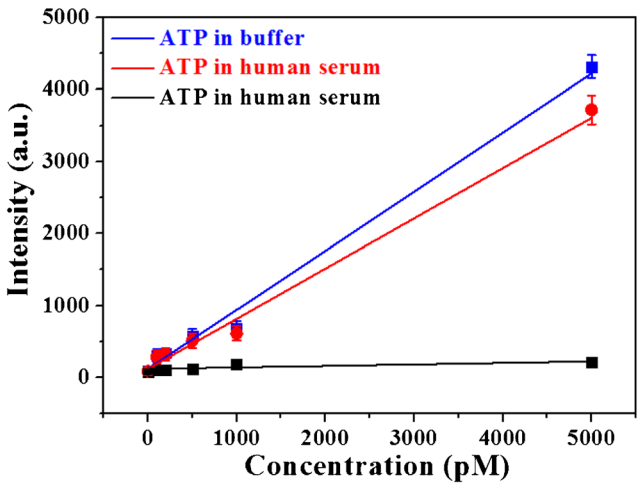

Fig. 6 The comparative results for the detection of ATP in buffer and human serum with different concentrations (100, 200, 500, 1000, 5000 pM). The SERS signal of the reaction platform without ATP in the human serum was used as a reference experiment (blue line)

Table 1 Practical analysis of ATP in human serum

Sample No.	Real value (pM)	Recovery (%)	RSD (%)
1	100	92.6	3.9
2	200	94.3	4.1
3	500	89.6	2.4
4	1000	90.1	3.2
5	5000	85.7	6.4

concentrations were between 85.7%–94.3%, and the RSD values were also obtained, implying good repeatability.

Conclusion

We present a new approach to selective SERS detection of ATP by aptamers-modified sandwich GO/AuNP nanolayer and AuNP monomer. The electric field intensity supported by our sandwich structure was one order of magnitude higher than that of single GO/AuNP nanolayer and gold nanoparticles, which indicated that this structure provided strong electromagnetic field coupling for SERS. Also, this result indicated that the sensitivity for SERS detection of ATP has been improved with the assistance of the split aptamers. In addition, other similar structures, such as GTP and CTP were used as controls to verify the detection specificity of ATP with our strategy. Due to this new configuration, the detectable concentration range of this aptamer-sensor was as low as 10 pM-10 nM, and the limit of detection was 0.85 pM. Therefore, we promise that this SERS-based platform can not only be widely used in the field of disease diagnosis, but also shows promising in other areas including the detection of pollutants and viruses [32, 33].

Acknowledgements This work was supported by the National Key Research and Development Program of China (2017YFB1104700), The Natural Science Foundation of China (NSFC, 21404015, 61774155, 61705227) and Jilin Science and Technology Department Project (20150204019GX).

Compliance with ethical standards

The author(s) declare that they have no competing interests.

References

1. Palleros DR, Raid KL, Shi L, Welch WJ, Fink AL (2018) ATP-induced protein Hsp70 complex dissociation requires potassium but not ATP hydrolysis. Nature 365:664–666
2. Desai A, Verma S, Mitchison TJ, Walczak CE (1999) Kin I kinesins are microtubule-destabilizing enzymes. Cell 96:69–78
3. Gourine AV, Llaudet E, Dale N, Spyer KM (2005) ATP is a mediator of chemosensory transduction in the central nervous system. Nature 436:108–111
4. Jhaveri S, Rajendran M, Ellington AD (2000) In vitro selection of signaling aptamers. Nat Biotechnol 18:1293–1297
5. Kang Y, Hua Y, Ning D, Zhu GC, Zhua TF, Jiang NJ (2017) A novel SERS-based magnetic aptasensor for prostate specific antigen assay with high sensitivity. Biosens Bioelectron 94:286–291
6. Berkley S, Bertram K, Delfraissy JF, Draghia-Akli R, Fauci A, Hallenbeck C, Kagame MJ, Kim P, Mafubelu D, Makgoba MW (2010) The 2010 scientific strategic plan of the global HIV vaccine Enterprise. Nat Med 16:981–989
7. Wanunu M, Dadosh T, Ray V, Jin J, McReynolds L, Drndic M (2010) Rapid electronic detection of probe-specific microRNAs using thin nanopore sensors. Nat Nanotechnol 5:807–814
8. Qian X, Peng XH, Ansari DO, Yin GQ, Chen GZ, Shin DM, Yang L, Young AN, Wang MD, Nie S (2008) In vivo tumor targeting and spectroscopic detection with surface-enhanced Raman nanoparticle tags. Nat Biotechnol 26:83–90
9. Zhang ZY, Chen NC, Li SH, Battig MR, Wang Y (2012) Programmable hydrogels for controlled cell catch and release using hybridized aptamers and complementary sequences. J Am Chem Soc 134:15716–15719
10. Zuo XL, Xiao Y, laxco KWP (2009) High specificity, high specificity, electrochemical sandwich assays based on single aptamer sequences and suitable for the direct detection of small-molecule target. J Am Chem Soc 131:6944–6945
11. Lim DK, Jeon KS, Hwang JH, Kim H, Kwon S, Suh YD, Nam JM (2011) Highly uniform and reproducible surface-enhanced Raman scattering from DNA-tailorable nanoparticles with 1-nm interior gap. Nat Nanotechnol 6:452–460
12. Joseph V, Engelbrekt C, Zhang JD, Gernert U, Ulstrup J, Kneipp J (2012) Characterizing the kinetics of nanoparticle-catalyzed reactions by surface-enhanced Raman scattering. Angew Chem Int Ed 51:7592–7596
13. Banholzer MJ, Millstone JE, Qin L, Mirkin C (2008) Rationally designed nanostructures for surface-enhanced Raman spectroscopy. Chem Soc Rev 37:885–897
14. Xu W, Ling X, Xiao J, Dresselhaus MS, Kong J, Xu H, Liu Z (2012) Surface enhanced Raman spectroscopy on a flat graphene surface. Proc Natl Acad Sci U S A 109:9281–9286
15. Kleinman SL, Ringe E, Valley N, Wustholz KL, Phillips E, Scheidt KA, Schatz GC, Van DRP (2011) Single-molecule surface-enhanced Raman spectroscopy of crystal violet Isotopologues: theory and experiment. J Am Chem Soc 133:4115–4122
16. Brown LV, Zhao K, King N, Sobhani H, Nordlander P, Halas NJ (2013) Surface-enhanced infrared absorption using individual cross antennas tailored to chemical moieties. J Am Chem Soc 135:3688–3695
17. Fan Z, Kanchanapally R, Ray PC (2013) Hybrid graphene oxide based ultrasensitive SERS probe for label-free biosensing. J Phys Chem Lett 4:3813–3818
18. Barhoumi A, Zhang DM, Tam F, Halas NJ (2008) Surface-enhanced Raman spectroscopy of DNA. J Am Chem Soc 130: 5523–5529
19. Braun G, Lee SJ, Dante M, Nguyen T, Moskovits M, Reich N (2007) A heterogeneous PNA-based SERS method for DNA detection. J Am Chem Soc 129:6378–6379
20. Lu G, Li H, Liusman C, Yin Z, Wu S, Zhang H (2011) Towards low-cost flexible substrates for nanoplasmonic sensing. Chem Sci 2:1817–1826
21. Huang J, Zhang L, Chen B, Ji N, Chen F, Zhang Y, Zhang Z (2010) Nanocomposites of size-controlled gold nanoparticles and graphene oxide: formation and applications in SERS and catalysis. Nanoscale 2:2733–2738

22. Loh KP, Bao Q, Eda G, Chhowalla M (2010) Nanocomposites of size-controlled gold nanoparticles and graphene oxide: formation and applications in SERS and catalysis. Nat Chem 2:1015–1024
23. Anker JN, Hall WP, Lyandres O, Shah NC, Zhao J, Van DRP (2008) Biosensing with plasmonic nanosensors. Nat Mater 7: 442–453
24. Fang N, Lee H, Sun C, Zhang X (2005) Sub-diffraction-limited optical imaging with a silver Superlens. Science 308:534–537
25. Qian XM, Zhou X, Nie SM (2008) Surface-enhanced Raman nanoparticle beacons based on bioconjugated gold nanocrystals and long range Plasmonic coupling. J Am Chem Soc 130:14934–14935
26. Hummers WS, Offeman RE (1958) Preparation of graphitic oxide. J Am Chem Soc 80:1339–1339
27. Qian XM, Li J, Nie SM (2009) Bimetallic nano-mushrooms with DNA-mediated interior nanogaps for high-efficiency SERS signal amplification. J Am Chem Soc 131:7540–7541
28. Qiu XJ, You XR, Chen X, Chen HL, Dhinakar A, Liu SG, Guo ZY, Wu J, Liu ZM (2017) A new interval-valued 2-tuple linguistic Bonferroni mean operator and its application to multiattribute group decision making. Int J Nanomedicine 12:4349–4360
29. Lal S, Grady NK, Goodrich GP, Halas NJ (2006) Profiling the near field of a Plasmonic nanoparticle with Raman-based molecular rulers. Nano Lett 6:2338–2343
30. Zhou CY, Wu CT, Liu YQ, Wang EK (2016) Effective construction of a AuNPs–DNA system for the implementation of various advanced logic gates. RSC Adv 6:106641–106647
31. Zhang X, Servos MR, Liu JW (2012) Instantaneous and quantitative functionalization of gold nanoparticles with thiolated DNA using a pH-assisted and surfactant-free route. J Am Chem Soc 134:7266–7269
32. Akki SU, Werth CJ (2018) Critical Review: DNA aptasensors, Are they ready for monitoring organic pollutants in natural and treated water sources? https://doi.org/10.1021/acs.est.8b00558
33. Su Y, Xu HG, Chen YH, Qi JX, Zhou X, Ge R, Lin ZK (2018) Real-time and label-free detection of bisphenol a by an ssDNA aptamer sensor combined with dual polarization interferometry. New J Chem 42:2850–2856